RFID Tag Antenna-Based Sensing for Pervasive Surface Crack Detection

Prasanna Kalansuriya, *Student Member, IEEE,* Rahul Bhattacharyya, *Member, IEEE,* and Sanjay Sarma, *Member, IEEE*

***Abstract*—We introduce the concept of using an RFID tag's antenna to sense surface cracks. Our contribution is two fold. First, we present the design of an inductively coupled loop antenna that can be used as a crack detector. Second, we propose the development of a 2-D grid of tags to improve spatial coverage and discuss how it can be used to monitor typical crack patterns in civil infrastructure. We demonstrate that the technique works reliably over a read distance of 1 m and in different types of environments. Potential engineering extensions and future research directions are also discussed.**

***Index Terms*—UHF RFID, antenna-based sensing, surface crack detection**

I. Introduction

The formation and propagation of surface cracks in civil infrastructure compromises the integrity of load bearing structures. The tragic collapse of Bridge 9340 in Minnesota in 2007, highlights the need for technologies that detect the onset of failure cracks in over-stressed structural elements [1]. Cracks are especially dangerous in brittle and inhomogeneous construction materials like concrete. A crack monitoring sensor should be able to predict the length and orientation of a crack. This is because factors such as crack length and orientation are known to affect the load bearing properties of structural materials [2]. Furthermore, the formation of cracks facilitates moisture ingress which can corrode steel reinforcement bars. Therefore, there is a strong motivation for pervasive crack detection especially in those zones most prone to structural failure as determined by limit state concrete design [3].

In this paper, we present the design of a UHF RFID crack detection sensor that is capable of estimating crack length and orientation at very low cost. There has been a lot of recent interest in using RFID tags for object identification purposes. RFID tags can be mass-produced at very low cost [4] and offer several advantages over competitive technologies, such as the bar-code, in terms of non-line of sight operations, improved read range and automated inventory management [5]. The opportunity to extend this wireless communication medium for pervasive sensing in structural health monitoring presents itself. We propose a sensor design and demonstrate how the position, length and orientation of a crack can be related to a change in the backscatter signal of the tag-sensor.

The rest of the paper is organized as follows. Section II compares and contrasts related work in crack detection with our approach. Section III presents the transduction principle and demonstrates how a crack is related to a change in the electrical properties of an RFID tag's response. Section IV extends this principle for pervasive monitoring of a surface. Section V then evaluates the performance of the sensor in different environments and for different read distances. Finally, Section VI presents a summary of the lessons learned and outlines the scope for future work.

The authors are with the Auto-ID Labs, Massachusetts Institute of Technology, Cambridge, MA, 02139 USA e-mail: prasanna, rahul_b and sesarma@mit.edu

II. Related Work

There have been several different approaches to surface crack detection in structural engineering. For instance, Zhang *et.al* have developed a smart film to detect the presence and location of surface cracks [6]. Their technique consists of embedding a mesh of conductive wires in a fabric that is bonded to the surface of a structure. Surface cracking propagates to the smart film and severs the corresponding wires in the mesh. The length and location of the crack can then be determined by detecting which wires have been severed. The authors experimentally verify that the smart film can be reliably used to detect crack length and position. In an extension to their work [7], the authors also discuss how the smart film technology can be fabricated using low-cost materials thus enabling pervasive sensor deployment. Similar work using capacitance changes [8] and the piezoresistive effect of carbon nanotube impregnated composites [9] have been reported for pervasive crack detection in the literature. However, these crack sensing techniques make use of lead wiring for data extraction. The placement and maintenance of large lengths of cabling wire is cumbersome and expensive.

Recently, there has been interest in developing pervasive sensors using RFID tags. RFID tags have seen large-scale, highly integrated deployment for object identification particularly in the supply chain and apparel industry. As a result, RFID tags today can be mass produced at very low costs. Furthermore, the communication protocols between the RFID tag and the reader are standardized and efficient [10], making RFID an ideal wireless communication infrastructure for pervasive sensing. In previous work, we've demonstrated how an RFID tag's antenna can be used as a sensor and related changes in some physical parameter of interest to a change in RFID tag response signal strength and frequency. Applications in displacement, temperature threshold and fluid level sensing were demonstrated [11], [12]. Similarly, other researchers have demonstrated how an RFID tag's antenna can be used to sense moisture [13] and volatile organics [14].

Occhiuzzi *et.al* presented the design of a meander line UHF RFID tag antenna that could be reliably used to measure axial strain. The axial strain changed the geometry of the antenna and this could be related to a change in the backscatter power of the RFID tag [15]. The authors presented the design of three tag antennas offering trade-offs between dynamic range and sensitivity. While the sensor is well suited for axial strain measurements, the direct application of this sensor to monitor cracking or bending strains in structural members is not immediately apparent. Similarly, Yi *et. al* demonstrated the design of an RFID patch antenna that relates strain to a change in tag operating frequency [16]. The authors demonstrated that the sensor can be reliably used to monitor strain up to 50 micro strain precision and over a read distance of a few feet. However, the sensor is based on a microstrip patch antenna design that makes use of vias to connect the antenna copper trace to the ground plane. This would increase the fabrication cost of the sensor as compared to a planar dipole like structure.

Our approach uses the RFID tag's antenna as a crack detector. We present the design of a grid made up of RFID tags. As a crack develops it severs some of the antennas in the grid permanently changing their impedance and radiation characteristics. This manifests itself as a drop in the backscatter signal responses of the affected tags. By detecting which tags register an abrupt drop in performance, we can infer the length and orientation of the crack. In the following sections, we discuss the design of such a grid. We also examine the robustness of the grid in different environments and for different read ranges.

III. Sensing Principle

An antenna-based crack sensor works on the principle that the presence of a crack permanently changes the radiation and impedance characteristics of the antenna. It is advantageous to choose an antenna design which has two properties. First, as soon as a crack severs the antenna it manifests itself in an abrupt change in antenna impedance. In other words, we need to ensure that a crack detunes the antenna. Second, depending upon the position of the crack along the antenna length the extent of detuning is more or less severe. The presence and location of a crack along the antenna can then be related to the drop in signal response of the RFID tag.

We make use of an inductively coupled loop antenna design proposed by Son and Pyo [17]. Here the radiating element is the crack detector and is fabricated by applying conductive paint directly on the surface to be monitored. The inductive loop, bearing the RFID chip, is fabricated using copper or aluminum foil. Fig 1(a) illustrates the dimensions of a tag designed for best performance on a cardboard sheet. The dipole length of 160 mm is chosen for two reasons. First, it is well suited for the 915 MHz operating frequency. Second, it presents a relatively long length over which cracks can be monitored.

The physics of crack detection may be understood by referring to the Friis transmission equation for radiative power transfer in the far field. Consider a reader-tag system, as shown in Fig 2, with a reader-tag separation of d and a reader

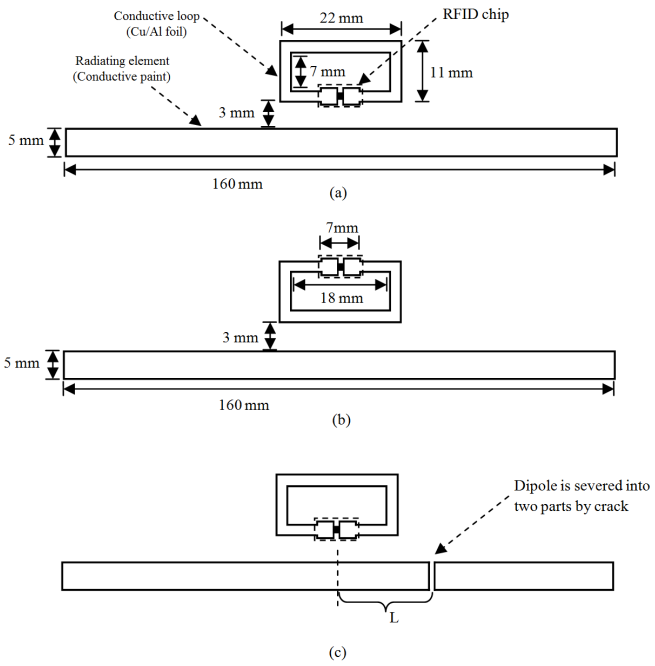

Fig. 1. (a) RFID tag type A; chip facing toward the dipole (b) RFID tag type B; chip facing away from dipole (c) Dipole of type A RFID tag is severed by a crack at a distance L from its center

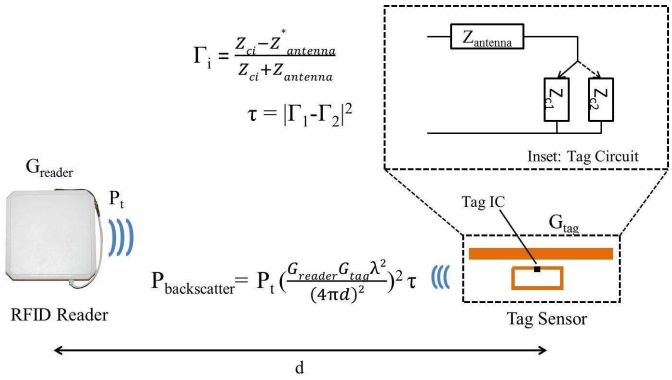

Fig. 2. Differential backscatter power from an RFID tag-sensor

transmitted power of P_t. The tag's antenna scavenges the incoming power and uses it to power the tag's IC. The tag's IC has two impedance states, Z_{c1} and Z_{c2}. Z_{c1} is typically well matched to the antenna impedance, $Z_{antenna}$. When Z_{c1} is presented as a load to $Z_{antenna}$, almost all the incoming power is transferred to the IC. Z_{c2}, is typically an open or short circuit and poorly matched to $Z_{antenna}$. When Z_{c2} is presented as a load to $Z_{antenna}$, almost all the incoming power is reflected. By switching between Z_{c1} and Z_{c2}, the tag amplitude modulates ID information back to the reader. The differential backscatter power corresponding to the signal strength of the RFID tag is a function of the difference between Z_{c1} and Z_{c2} and is given by [18]:

$$P_{backscatter} = P_t \left(\frac{G_{tag} G_{reader} \lambda^2}{(4\pi d)^2} \right)^2 \tau \qquad (1)$$

where G_{tag} and G_{reader} are the tag and reader antenna gains, λ is the carrier wavelength and τ is the power transmission coefficient which depends upon how well the two chip impedance states are *matched* to the antenna impedance:

$$\tau = |\Gamma_1 - \Gamma_2|^2 \quad (2)$$

$$= \frac{4R_{antenna}R_{chip}}{|(R_{antenna}+R_{chip})^2+(X_{antenna}+X_{chip})^2|} \quad (3)$$

where $R_{antenna}$ and R_{chip} are the resistive components of the antenna and chip impedance while $X_{antenna}$ and X_{chip} are the reactive components of the antenna and chip impedance. It is easy to see that when $R_{antenna}$=R_{chip} and $X_{antenna} = X^*_{chip}$, $\tau = 1$ and the tag responds with the best signal strength.

Referring to Eq. 1, we observe that G_{tag} and τ are dependent on the integrity of the radiating element. If a crack develops at a location L as highlighted in Fig 1(c), the radiating length of the antenna is shortened which manifests itself as a change in the antenna impedance and tag radiation pattern. Therefore both τ and G_{tag} are functions of the crack location, L:

$$\tau(L) = \frac{4R_a(L)\,R_c}{\left((R_a(L)+R_c)^2+(X_a(L)+X_c)^2\right)} \quad (4)$$

$$G_{tag} = f(L) \quad (5)$$

Let G_0 and τ_0 be the tag antenna gain and power transfer coefficient respectively for a tag having a healthy unaffected radiating element. Using (1) and (2) the difference in backscatter power in dB between the healthy and cracked states of the sensor can be expressed as,

$$\Delta P_{backscatter}(dB) = 20log\left(\frac{G_{tag}(L)}{G_0}\right) + 10log\left(\frac{\tau_L}{\tau_0}\right) \quad (6)$$

We simulate the presence of a single crack using an appropriate finite element solver [19], and vary its position from $L = -8cm$ to $L = 8cm$ along the radiating element. We also note that the loop element of the antenna is capable of being placed in two orientations (c.f Fig 1(a) and Fig 1(b)) and we examine the effect of both orientations in our simulations.

Fig 3 presents the simulated values of $\Delta P_{backscatter}$ between the cracked and uncracked states of the sensor for different crack locations and for both orientations of the inductive loop. We observe that the drop in tag performance is significant for $L = -4cm$ to $L = 4cm$. Furthermore, the drop in performance is sharper for the inductive loop oriented as seen in Fig 1(a). We therefore proceed with the *Type A* tag in our study.

To verify the accuracy of our simulations, we then subject the tag to an experimental test. We conduct the test for a reader-tag separation of 75 cm in a laboratory room with no special anechoic provisions and using the Impinj Revolution RFID reader [20] set to transmit at a maximum power of 36 dBm EIRP. For each crack location, L, at least 50 measurements were taken and mean and standard error values were reported. As observed Fig 4, there is good correspondence between the experimental and simulated results.

We note from Fig 4, that there is a measurement uncertainty

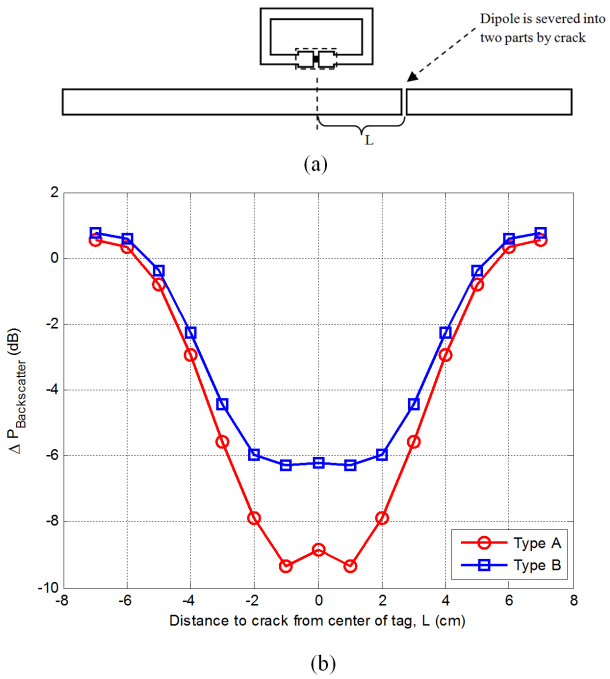

Fig. 3. Difference in the received power ($\Delta P_{Backscatter}$) of the two states, healthy and cracked, against the distance to the crack location, L, measured from the center of the tag. (a) Illustration of the crack location (b) $\Delta P_{Backscatter}$ against L for the two different tag types A and B.

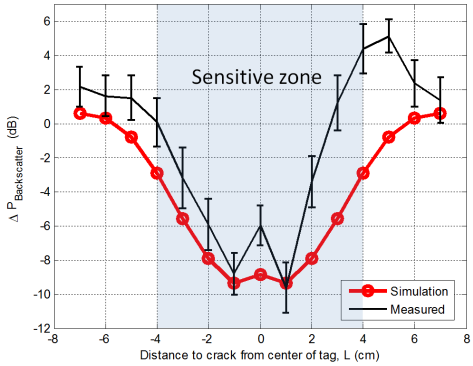

Fig. 4. Comparison of the simulated and measured $\Delta P_{backscatter}$ against the distance to the crack location, L, in a type A tag.

of 2-3 dB associated with the tag power measurements. There are two reasons for this. First, the experiment was conducted without any anechoic provisions and thus measurements are affected by multi-path noise. Second, the RFID reader implements FCC mandated frequency hopping [18] in the 902-928 MHz band which causes slight variations in τ. On the basis of this observation, we can conclude that the tag-sensor is sensitive to cracking between $L = -4cm$ and $L = 4cm$ where the mean signal drop is significantly higher than the measurement uncertainty.

We conclude that the radiating element can indeed be used as a crack detector, however is sensitive to cracking in the middle half of the radiating element. It is important to

consider how this sensing technique can be extended to cover larger surface areas by making use of an antenna grid. This discussion is the subject of the next section.

IV. Design of a Crack Sensing Array

In the previous section, we demonstrated the feasibility of crack sensing using the inductively coupled loop antenna. We also demonstrated that the radiating element is sensitive to cracking only in $L = -4cm$ to $L = 4cm$ zone. In order to extend the zone over which a crack is detected, we make use of a grid of RFID tags. First, we discuss the design of a 1-D grid to detect crack position along a line. Next, we extend the 1-D grid to a 2-D grid to detect cracks in an area.

A. Linear array

We present a simple 1-D grid by creating two rows of RFID tags closely separated from one another as shown in Fig 5. The tags in one row are staggered with respect to the tags in the other row so that the sensitive zones of one tag cover the insensitive zones of another tag. For instance, for the crack shown in Fig 5, the crack occurs in the insensitive zone of tag 1, but in the sensitive zone of tag 2.

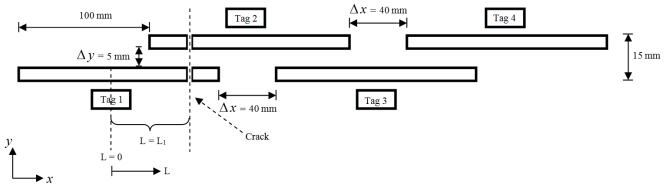

Fig. 5. Linear array of sensors

It is essential to verify that the grid performs as anticipated. This is because RFID tags in close proximity with one another tend to couple and this may cause unpredictable variations in performance [21]. The proximity between tags in both x and y directions will introduce coupling. In order to implement a linear array Δy needs to be small. It was found experimentally that a spacing of 0.5 cm gives acceptable performance. Δx was chosen to be 4 cm. In order to verify that coupling does not unduly affect performance, we simulate the performance of the 1-D grid when it is subjected to a single crack between $L = 0cm$ and $L = 30cm$. The results are plotted in Fig 6(a). We observe that it is possible to infer the presence of a crack by observing a drop in signal of tags 1 to 4. However, we also note the presence of dead zones which are cases where neither of two adjacent sensors registers a significant drop in signal performance. Therefore, a crack would be missed in these zones. In this paper, we don't attempt to optimize the 1-D grid but acknowledge its limitations as an avenue of future investigation. Experimental results observed in Fig 6(b) show close correspondence with the simulated results.

B. 2-D Array

We monitor a 2-D area by replicating the linear array, discussed in Section IV-A, in the second dimension as shown

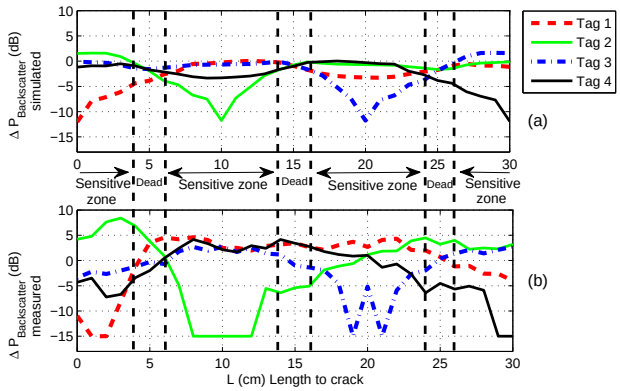

Fig. 6. (a) Simulated $\Delta P_{backscatter}$ of linear sensor array (b) Measured $\Delta P_{backscatter}$ of linear sensor array

in Fig 8. We choose an inter-array separation of $\Delta y = 5cm$ as a compromise between maximizing the coverage area while accommodating all the radiating elements and inductive loops. Also in order to reduce the size of the dead zones in the individual linear arrays we have reduced Δx to 2 cm. It was verified through simulations that this reduction does not affect the sensitive zone profile as shown in Fig. 7. Since the sensitive zone spans 8 cm wide (Refer Fig. 4) the new arrangement reduces the width of each of the dead zones to 1 cm.

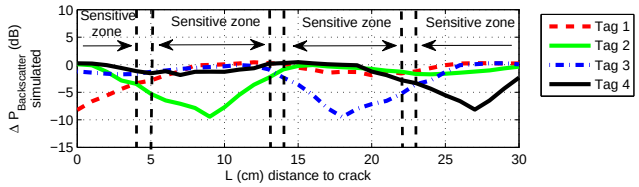

Fig. 7. Simulated $\Delta P_{Backscatter}$ of linear sensor array with $\Delta x = 2$ cm

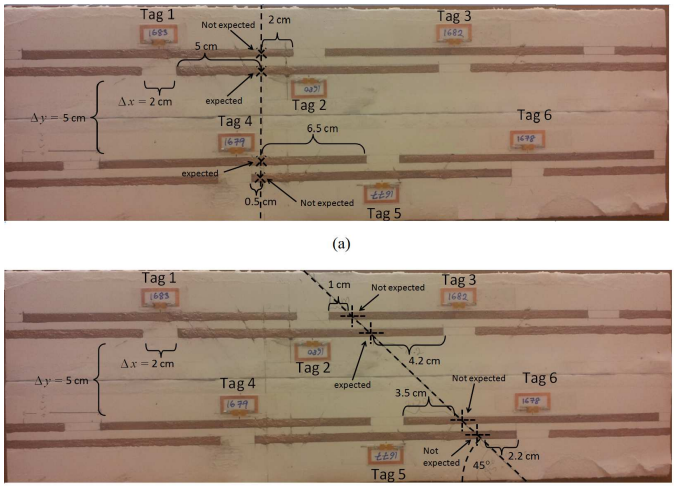

Fig. 8. Space filling array of sensors. The dipole is painted on the structure using conductive ink and the loop is made of adhesive copper tape. (a) Emulation of straight crack propagation and (b) angular crack propagation. The tags where a change in RSSI is expected or not expected are also marked.

In this case, we directly verify the 2-D array's performance by subjecting it to tests. Fig. 8 shows the 2-D array constructed for testing the system performance for different cracks. Fig. 9 illustrates the performance of the array when it is subject to a straight and angular crack. The experiment was conducted at a reader-grid separation of 50 cm. The figure shows the change in the received signal strength indicator (RSSI) in dB between the healthy state and the cracked state of the structure for each tag (1 to 6) deployed in the 2-D array.

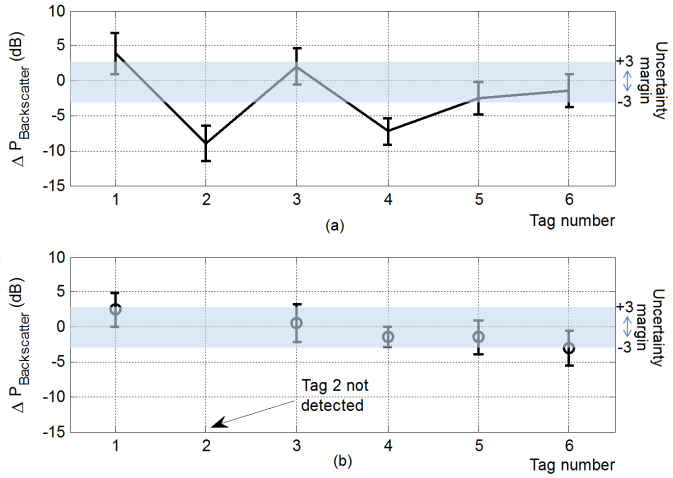

Fig. 9. Change in RSSI for the emulated cracks shown in Fig. 8 (a) straight crack (b) angular crack. In the case of the angular crack tag 2 is not detected due to the signal drop being too severe.

From Fig. 9 we see that there is a sharp change in the RSSI for tags 2 and 4 for the straight crack, in excess of 5 dB. Which is in accordance with the crack propagation shown in Fig. 8 (a) where the crack severs the radiating element of tags 2 and 4 in the high sensitivity region. For the angular crack we observe that only tag 2 registers a large change in RSSI where it is completely detuned because of the crack and is not detected by the RFID reader. This observation also agrees with the crack propagation shown in Fig. 8 (b) where the 45^0 angular crack is closest to the inductive loop of tag 2. From Fig.9, we observe some interesting side effects as a result of cracking. For instance, in Fig 9(a), tags 1 and 3 demonstrate a marginal improvement in performance on cracking whereas tag 6 registers a slight drop in performance. Similarly, referring to Fig. 9(b), tag 1 registers a slight improvement in performance while tag 4 registers a slight drop in performance. We attribute these effects to the complex interaction/coupling between the tags in the 2-D array. In addition, the average signal improvement/reduction is within the 2-3 dB uncertainty margin associated with measurements.

We observe that the 2-D array performs exactly as per specifications and it is possible to infer both the presence and propagation of the straight crack and in the event that the crack is not propagating through sensitive zones, as in the case of the angular crack, it is still possible to detect the fact that a crack has occurred and that a maintenance inspection is warranted.

C. Practical Deployment of the 2-D Array

While Section IV-B illustrates the feasibility of crack sensing using RFID, the dead zones in the linear array and the inter-array separation cause gaps in the detection grid. Fig. 10 represents an equivalent grid representation of the 2-D array. As long as a crack severs the labeled sensitive zones, the crack is detected.

With this information, we can deploy a health monitoring strategy for concrete structures by deploying the 2-D grid in zones most susceptible to structural damage. For instance, Fig. 11 (a) and Fig. 11 (b) highlights how the 2-D grid could be used to monitor shear and flexural cracking zones in reinforced concrete beams.

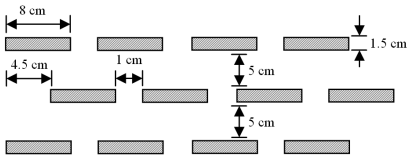

Fig. 10. Equivalent grid representation of the high sensitive zones of the 2-D array shown in Fig. 8. As long as a crack passes through the grey zones it will be detected.

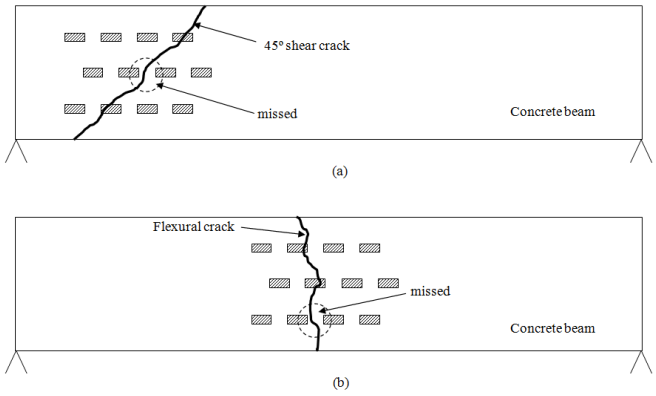

Fig. 11. Usage of 2-D grid for monitoring (a) shear and (b) flexural cracking zones in reinforced concrete beams. The locations where the propagating crack has missed a sensitive zone are also highlighted.

V. Results of Laboratory Testing

To determine the universal applicability of this technique, we subject the 2-D grid to tests in two different types of environments — an open room and a room filled with tables, boxes, metallic cabinets and other sources of clutter. In each environment, we perform the test at different reader-tag separations. Fig. 12 shows the results for two types of crack propagation in the two different environments for different reader-grid separations. For the case of the straight crack propagation it is clear (as shown in Fig. 8 (a)) that the crack is propagating through the two RFID tags 2 and 4. These two tags show a change in RSSI greater than 5 dB under all conditions considered in the experiments which clearly implies that they are affected by a crack. For the angular crack propagation (refer Fig. 8 (b)) only tag 2 is affected by the crack and shows

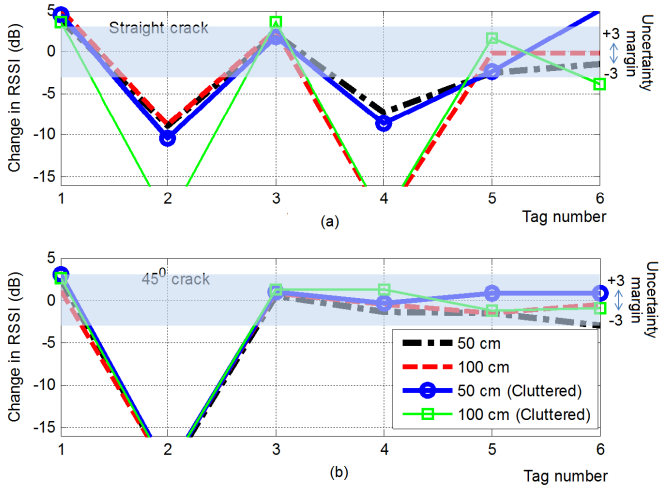

Fig. 12. Change in RSSI for (a) straight and (b) angular crack propagation in two environments for different distances. Changes in RSSI exceeding -15 dB are cases where the tag was not detected due to received signal strength being lower the RFID reader sensitivity.

a larger change in the RSSI. It should be noted that in some cases (for the angular crack and when reading the sensor at larger distances) the tags were detuned by the cracks to an extent that they were not picked up the RFID reader.

VI. Conclusion and Future Work

In this paper, we introduced the concept of surface crack sensing using ordinary RFID tags. We started by demonstrating the feasibility of using an inductive loop coupled antenna for crack sensing. We observed that the antenna was sensitive to cracking only for 50% of the radiating element's length. We then proposed extending this concept to a linear and 2-D array. We demonstrated that the technique worked reliably for different reader-tag separations and in different environments. However there are still gaps in the detection grid where a crack could be missed. Finally, we highlighted how this sensing concept could be used to monitor the zones in concrete structures most susceptible to structural damage.

We can classify future steps along two broad areas — open research questions and engineering problems. With regards open research questions, it is important to further optimize the sensor grid's spatial resolution. This involves reducing the dead zones in the linear array and devising techniques to reduce the inter-array separation in the 2-D array. Second, it is important to investigate the effect of crack width on sensor performance. In our tests, we have assumed cracks that are 1-2 mm wide that cause an observable break in the radiating element. It is essential to investigate the effect of thinner cracks — such as micro cracks — on the grid performance. Finally, we have assumed that a crack in the concrete surface severs the radiating element as it propagates. In practice the elasticity of the conductive paint, and the concrete-paint bond strength may influence the ability of the radiating element to rupture. Laboratory tests on concrete samples need to be conducted to investigate this question further.

Enhancing the read distance of the 2-D grid is an open engineering challenge. Through experiments, we note that the 2-D grid works reliably for a reader-tag separation of 1 m. In practice, these sensors will be read by reader equipment deployed on passing maintenance vans so a read range of 3-4 m is required. This could be achieved by considering several techniques such as using directional reader antennas and using semi-passive tags to create the sensing grid.

References

[1] R. Holt and J. Hartmann, " Adequacy of the U10 & L11 Gusset Plate Designs for the Minnesota Bridge No. 9340 (I-35W over the Mississippi River)," National Transportation and Safety Board, Tech. Rep., 2008.
[2] J. Zhang, V.C Li and H. Stang, "Size Effect on Fatigue in Bending of Concrete," *Journal of Materials in Civil Engineering*, vol. 13 No. 6, pp. 446–453, 2001.
[3] S. U Pillai and D. Menon, *Reinforced Concrete Design*. Tata McGraw Hill, 2003.
[4] S. Sarma, "Towards the 5 c tag," *Auto ID Center: White Paper*, 2001.
[5] M. Tajima, "Strategic value of RFID in supply chain management," *Journal of Purchasing and Supply Management*, vol. 13 No 4., pp. 261–273, 2007.
[6] B. Zhang, Z. Zhou, K. Zhang, G. Yan and Z. Xu, "Sensitive Skin and the Relative Sensing System for Real-time Surface Monitoring of Crack in Civil Infrastructure," *Journal of Intelligent Material Systems and Structures*, vol. 17, pp. 907–917, 2006.
[7] Z. Zhou, B. Zhang, K. Xia, X. Li, G. Yan and K. Zhang, "Smart film for crack monitoring of concrete bridges," *Structural Health Monitoring*, vol. 10 No. 3, pp. 275–289, 2011.
[8] S. Laflamme, M. Kollosche, J.J Connor and G. Kofod, "Soft capacitive sensor for structural health monitoring of large-scale systems," *Structural Control and Health Monitoring*, vol. 19 No. 1, pp. 70–81, 2012.
[9] K. J Loh, T. C Hou, J. P Lynch and N. A Kotov, "Nanotube-based Sensing Skins for Crack Detection and Impact Monitoring of Structures," *Proceedings of the International Workshop on Structural Health Monitoring*, p. 16851692, 2007.
[10] EPC Global, "Class 1 Generation 2 UHF Air Interface Protocol Standard," *http://www.epcglobalinc.org/standards/uhfc1g2*.
[11] R. Bhattacharyya, C. Floerkemeier and S. Sarma, "Low Cost, Ubiquitous RFID Tag Antenna Based Sensing," *Special Issue of IEEE Proceedings: RFID - A Unique Radio Innovation for the 21st Century*, vol. 98 No. 9, pp. 1593–1600, 2010.
[12] R. Bhattacharyya, C. Floerkemeier, S. Sarma and D. Deavours, "RFID Tag Antenna Based Sensing in the Frequency Domain," *IEEE International Conference on RFID*, pp. 70–77, 2011.
[13] J. Siden, X. Zeng, T. Unander, A. Koptyug and H.E. Nilsson, "Remote Moisture Sensing utilizing Ordinary RFID Tags," in *IEEE Sensors*, Oct. 2007, pp. 308 –311.
[14] R.A Potyrailo, C. Surman,W.G Morris, S. Go, Y. Lee, J. Cella and K.S Chichak, "Selective quantitation of vapors and their mixtures using individual passive multivariable RFID sensors," in *IEEE International Conference on RFID*, April 2010, pp. 22 –28.
[15] C. Occhiuzzi, C. Paggi and G. Marrocco, "Passive RFID Strain-Sensor Based on Meander-Line Antennas," *IEEE Transactions on Antennas and Propagation*, vol. 59 No.12, pp. 4836–4840, 2011.
[16] X. Yi, T. Wu, Y. Wang, R. T Leon, M. M Tentzeris and G. Lantz, "Passive Wireless Smart-Skin Sensor using RFID-Based Folded Patch Antennas," *International Journal of Smart and Nano Materials*, vol. 2 No. 1, pp. 22–38, 2011.
[17] H. W. Son and C. S. Pyo, "Design of RFID tag antennas using an inductively coupled feed," *Electronics Letters*, vol. 41 No. 18, pp. 994–996, 2005.
[18] Daniel M. Dobkin, *The RF in RFID: Passive UHF RFID in Practice*. Newton, MA, USA: Newnes, ©2007.
[19] Complete Technology for 3D EM Simulation. [Online]. CST Computer Simulation Technology AG. Darmstadt, Germany. Available: http://www.cst.com/. [Online]. Available: http://www.cst.com/
[20] Impinj Speedway®Revolution RFID Reader with AutoPilot Features. http://www.impinj.com/Speedway_Revolution_UHF_RFID_Reader.aspx.
[21] G. Marrocco, "RFID Grids: Part 1 — Electromagnetic Theory," *IEEE Transactions on Antennas and Propagation*, vol. 59, no. 3, pp. 1019 –1026, march 2011.